

Deformable Wheel Robot Based on Origami Structure

Dae-Young Lee, Gwang-Pil Jung, Min-Ki Sin, Sung-Hoon Ahn and Kyu-Jin Cho, *Member, IEEE*

Abstract— Origami is the traditional Japanese art of paper folding. Due to its fascinating properties, several attempts are being actively made to expand applications of origami-inspired designs in engineering. This paper presents the design of a deformable wheel based on an origami structure that was integrated with a small-scale mobile robot. The wheel of the robot employs an origami structure proposed by Guest *et al.* All segments of the structure are connected by links-i.e., folding lines-and this linked structure provides advantages in terms of maintaining geometry and force transmissibility. These two advantages enable control of the shape or size of the wheel by activating a certain portion of the structure. With this property, the wheel diameter of the robot is reduced from 11 cm to 4 cm by four SMA coil spring actuators. Two plate springs are embedded in the wheel to maintain stiffness and allow the wheel to recover from contraction. With the deformable wheel, the robot can pass through a 5 cm gap despite having an 11 cm wheel in its normal state. This deformable wheel concept can be used to build mobile robots that can move quickly with large wheels and move through small gaps when required.

I. INTRODUCTION

A robot with a deformable wheel has the potential to overcome different types of obstacles, from narrow gaps to high steps. There have been studies about deformable wheel to achieve these advantages [1]-[3]. The two important issues in deformable wheel design are building an effective wheel deforming mechanism and guaranteeing the stiffness in various states of the wheel. One approach that can provide a solution to these issues is to use origami concept.

Origami is the traditional Japanese art of paper folding. A paper can be folded into thousands of different three-dimensional shapes depending on the positions of the folding lines, order of folding, and way of the folding [4]. This fascinating property has attracted many artists and mathematicians [5]-[7]. Not only artists and mathematician, but engineers are also fascinated by these unique properties of origami and actively attempt to expand the application of origami designs in engineering [8]-[12].

Among the many studies on engineering applications of origami, some have suggested that origami structures can be treated as a mechanical mechanism [13]. Each fold line and vertex can be regarded to be a mechanical components-e.g.,

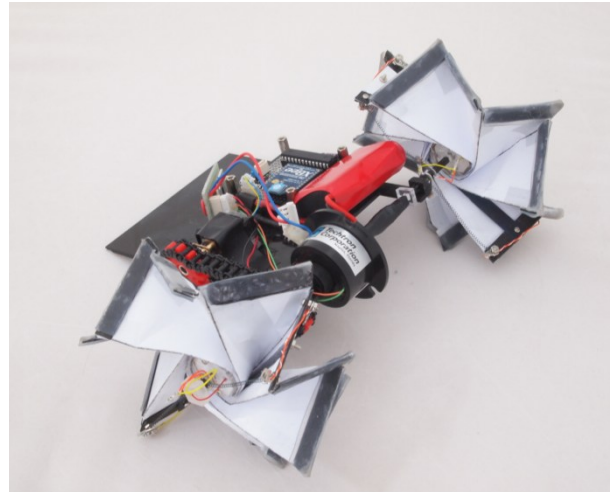


Figure 1. Deformable wheel robot

linkages and joints. By the same token, the origami itself could be treated as a combined structure of the mechanical components. It leads to the potential that it is possible to achieve a specific mechanical functionality by using specially design origami structure. As one case of verification of this idea, we used origami structure as a wheel with mechanism of radius change.

The characteristic of origami structure gives unique advantages. First, it enables prediction of movement of a morphing structure. In general, analyzing morphing or compliant structure requires pseudo-rigid modeling, numerical method or other kinds of approximation technics. The movement of origami-based morphing structures, however, can be estimated more exactly even in large deformation, and furthermore, it enables design for movement of the whole structure.

Second, it gives advantages in fabrication. Origami structures start from a two-dimensional layer and are transformed into three-dimensional structures through folding. The wheel structure is made from a two-dimensional patterning process and is transformed into the three-dimensional wheel by folding. The simplified assembly and manufacturing process not only reduces cost, time, and difficulty, but also increases the robustness of the system in aspect that small number of parts are used in mechanism. The structure is more affordable to large external impact and has less riskiness of unassembled. Friction and wearing between parts are also reduced.

In this paper, a novel concept of a deformable wheel robot using the origami structure is proposed. The wheel of the robot employs the origami structure proposed by Guest *et al* [14]. The origami structure is a linked structure and can maintain its stiffness and transmit forces through the links. These two

*Resrach supported by the National Research Foundation of Korea(NRF) (No. 2012-0000348)

D. Lee, G. Jung, M. Sin and S. Ahn are with the School of Mechanical and Aerospace Engineering, Seoul National University, Gwanak 1 Gwanak-ro, Gwanak-gu, Seoul 151-742, Korea (e-mail: winter2nf@gmail.com; gwangpiljung@gmail.com; smkch@nate.com; ahnsh@snu.ac.kr)

K. Cho is with School of Mechanical and Aerospace Engineering, Seoul National University, Gwanak 1 Gwanak-ro, Gwanak-gu, Seoul 151-742, Korea (phone: +82-2-880-1663; fax: +82-2-880-1663; email: kjcho@snu.ac.kr)

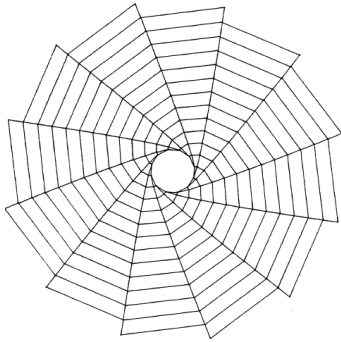


Figure 2. Designed folding pattern when the hub has 12 vertices. This model considers the thickness of membrane and uses vector calculus for patterning (Guest and Pellegrino, 1992).

advantages enable the shape or size of the wheel to be controlled through activation of a certain portion of the structure. The wheel is built using paper reinforced with carbon fiber at the edges and two plate springs are embedded in the wheel to maintain stiffness and allow it to recover from contraction. Four SMA spring actuators are installed for contraction. The diameter of the wheel is 11 cm in its normal state and reduced to 4 cm when contracted. This deformable wheel concept can be used to build mobile robots that can move quickly with large wheels and move through small gaps when required.

The following sections present the wheel structure, robot design, and experimental results. More details on the properties of the structure are discussed. The experimental results demonstrated the robot performance with regard to steering around and overcoming narrow gaps and various obstacles.

II. WHEEL DESIGN

A. Wheel Structure

The wheel structure design was derived from the model proposed by Guest *et al*, which was originally developed for folding inextensible space sail membrane [14]. Using vector calculus, the authors proposed folding pattern design method for a space sail membrane shown in Fig. 2 and 3. In this study, a wheel-folding pattern with a 12-vertex hub was used.

This structure has two main advantages. First is the shape maintenance; all of the wheel segments are linked together and enable the structure to maintain a circular shape independent of whether it is folded or not. This is one of the main reasons why this structure was selected to be used as a wheel. Second is the force transmissibility and the stiffness maintenance. A wheel that supports the entire body of the robot usually encounters a stiffness problem. How much weight the wheels can endure is the main issue of the wheel, and it is even more important for deformable wheel which usually has a certain degree-of-freedom for deformation. Since the entire wheel structure is linked together, controlling the stiffness of every segment is not required. The wheel stiffness can be easily controlled by controlling a certain portion of the structure. This property also reduces the number of actuators: that is, an actuator is not needed in every segment to control the entire structure. This reduces complexity of the system and increases the power efficiency when changing the shape.



Figure 3. Unfolded and folded shapes. Wheel body is made from paper and folded manually. Edge of wheel is reinforced by CFRP

B. Actuation Mechanism

There are two main issues that should be considered for actuation; maintaining stiffness of the wheel at a certain shape, and actuation. With regard to the first issue, the wheel should bear the weight of all components such as electronics, batteries, and transmission. To maintain the desired shape under the loading condition, a component to maintain stiffness is required to prevent the wheel from unwanted deformation. A pair of plate springs was used in the design for this purpose (Fig. 4). These two plate springs support and maintain the stiffness of the whole structure.

The other issue is how to actuate the wheel. Actuators for wheel deformation require a large linear stroke. In addition, a light-weight and simple structure is required for embedment. We used SMA coil spring actuators to satisfy these requirements. The four SMA spring actuators were installed symmetrically on each side (Fig. 4). One end was connected to the wheel axis, and the other was connected to the pin located at the end of the wheel.

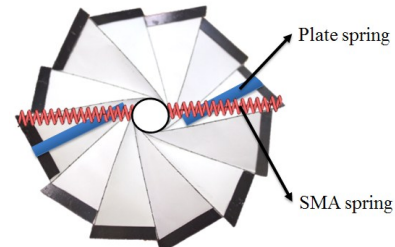


Figure 4. Schematic diagram of the wheel. SMA springs for contraction and plate springs for extension are installed.

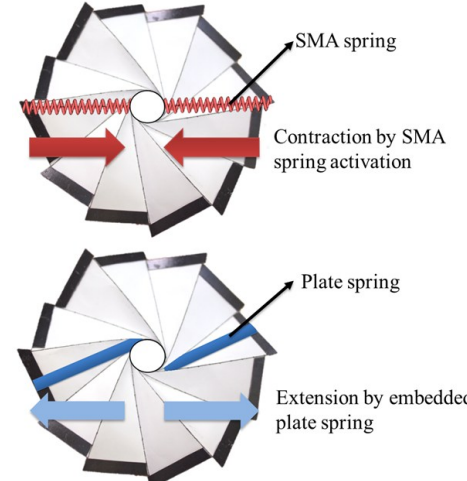


Figure 5. Concept of the wheel actuation mechanism. Contraction forces are generated by the SMA spring actuators and extension force are generated by the plate spring. Contraction is active actuation and extension is passive actuation.

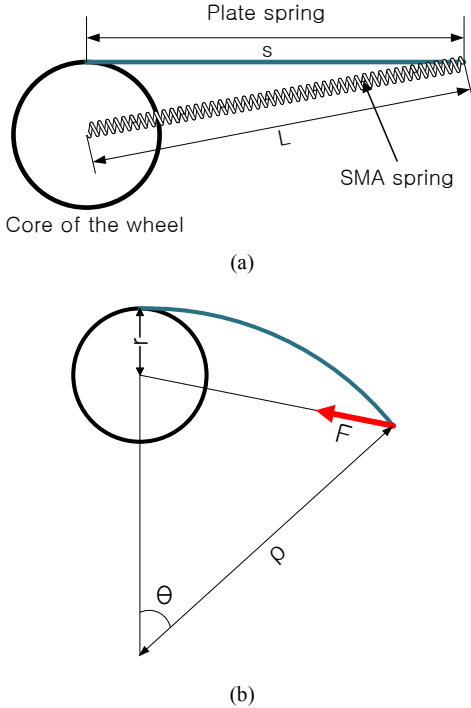


Figure 6. Simplified model of the origami wheel. The model was used to derive the relationship between the radius of the wheel (L) and force of the SMA (F). The model can be used to estimate the force required to deform the wheel.

The wheel actuation mechanism is simple. When the SMA actuators are activated, the SMA actuators pull the ends of the structure and it leads to contraction of the wheel. When the SMA actuators are deactivated, the plate springs extend the wheel to the original shape (fig. 5).

III. MODELING

In order to determine the design parameters of the SMA actuator, a model of the wheel is required. The wheel is an elastic body that can change diameter. For simplifying analysis of the wheel, some conditions are assumed. First, stiffness of the paper was neglected. The paper used in the wheel has relatively low small stiffness compared to the plate spring. Second, when a force is applied to the plate springs, it has same curvature in all sections. Third, the axial stress during bending was neglected. In the analysis, only the pure moment component was considered. Based on these assumptions, the model of the wheel was simplified as shown in Fig. 6 (a).

From the beam theory, eq. (1) is derived.

$$M = \frac{EI}{\rho} \quad (1)$$

where M is the applied momentum and E and I are the elastic modulus and moment of inertia, respectively, of the plate spring. ρ is the curvature of plate spring.

The momentum applied to the plate spring is

$$M = r \times F \quad (2)$$

where r is the radius of the core of the wheel and F is the applied force from the SMA spring actuator. From this equation, the relationship between F and ρ is,

$$F = \frac{EI}{r\rho} \quad (3)$$

From Fig. 6 (b), the relationship between ρ and L is derived geometrically

$$L^2 = \rho^2 + (\rho - r)^2 - 2\rho(\rho - r)\cos\theta \quad (4)$$

$$\theta = \frac{s}{\rho} \quad (5)$$

where s is the length of the plate spring and θ is the central angle of the plate spring.

From the above equations, the relationship between L and F is derived as

$$L^2 = r^2 + 2(\rho^2 - r\rho) \left\{ 1 - \cos\left(\frac{s}{\rho}\right) \right\} \quad (6)$$

$$L^2 = r^2 + 2 \left[\left(\frac{EI}{rF} \right)^2 - \frac{EI}{F} \right] \left\{ 1 - \cos\left(\frac{srF}{EI}\right) \right\} \quad (7)$$

where L is the radius of the wheel.

Because of the non-linearity between L and F , it is hard to solve this equation analytically. However, it still gives numerical data on the relationship between L and F . From this model, we can predict the force needed to deform the wheel and the tendency for diameter transition when force is applied.

IV. ROBOT DESIGN & FABRICATION

A. Wheel Material

We used paper to make the origami wheel. The important properties of the material used in an origami structure are the stiffness difference between facets and fold line and tendency of folding into the desirable direction. The paper characteristics corresponded to these two properties.

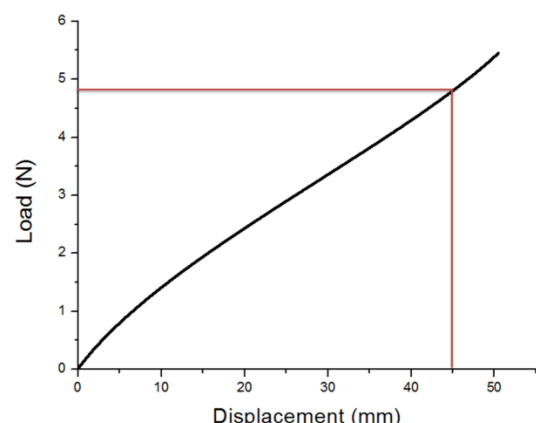


Figure 7. Relationship between the radius displacement and load using Eq. (7). Red lines indicate the target displacement and required force.

Carbon fiber reinforced plastic (CFRP) plates were added to the end segment of the wheel to reinforce the paper structure, and silicon polymers (Ecoflex) were added to the end segment of the wheel to increase the wheel friction.

B. Wheel Actuation

Fig. 7 plots the relationship between the radius displacement and load using Eq. (7) in section III. The constant values in the model were set from the robot design: s was 70 mm, r was 15 mm and EI was 1500 N · mm 2 . EI value was estimated from the three-point bending test. We set the target displacement to 45 mm, and from the graph, we determined that this required a force of less than 5N. Using this property, the design parameters of the SMA were determined. The actuator had an 8 mil wire diameter, 1mm spring diameter and 36 active coils. The spring constant k and deflection δ of the SMA coil actuator in the austenite phase are given by following equations:

$$\delta = \frac{8PD^3n}{Gd^4} \quad (8)$$

$$k = \frac{Gd^4}{8D^3n} \quad (9)$$

where D is the spring diameter, d is the wire diameter, P is the load, the shear modulus G of Ni-Ti in the austenite phase is 25 GPa, and the number of the active coil n is 36.

Fig. 8 shows the wheel fabrication results. Fig. 8 (a) shows the initial state. When the SMA actuators are activated, the wheel starts to deform as shown in Fig. 8 (b). After actuation, the wheel reaches its minimum size, which is 30% of the initial state. Inversely, the size of the wheel goes back to the initial state when the SMA actuators are cooled.

One important thing is the direction of the actuation force. The crimps at the end of the SMA actuators rotate freely at the pins and axis. Therefore, the direction of the actuation forces is always on the straight line between the axis and pins, which provides the structure with a continuous bending moment. Both ends of the SMA actuators are clamped with crimps, as shown in Fig. 9.

C. Electronics

Atmel's microprocessor Atmega8 was used to implement the control system. Atmega8 is an 8-bit micro controller and has 23 programmable I/O lines and 16 MHz clock speed. It was used in this study to control the motor and SMAs using PWM signals. A transistor (s9013) was used to drive a current to the motor and SMAs. Zigbee communication protocol was used for remote control, which is specialized for simple and low-power communication. A Zigbee module (XB24-ACI-001) is used and it communicates with the microprocessor using UART.

In order to ensure the safety of the microprocessor, power source of the SMAs and the motor were separated from the microprocessor. Both batteries were lithium polymer, and the battery voltage of SMAs and motors are selected high (3cell, 11.7V) due to efficiency [10].

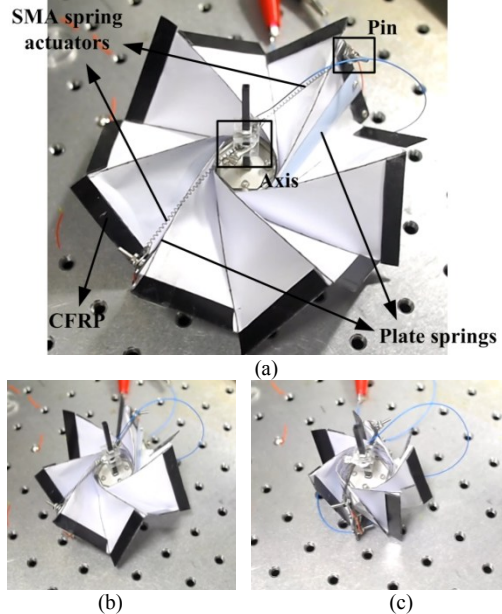


Figure 8. Origami deformable wheel: (a) initial state (b) middle state (c) final state. When current is applied to the SMA springs, they contract and deform the wheel size.

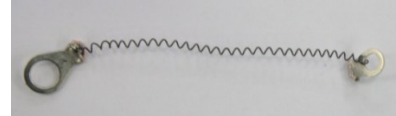


Figure 9. SMA spring actuator with crimps at the ends. The crimps freely move and rotate at the axis and pin.

The power transmission from body to wheel for SMAs was one of important design problem. The controller and batteries were on the body frame, and SMAs were on the rotating wheels. A slirpring was adopted to solve this power transmission problem. A Slirpring is electrical signal transmission tool between rotating and non-rotating parts. Techtron Corporation's SRA-73632-6 model was used. It provides six channel signals and can support 2 A for each channel. Its specifications were sufficient for the driving SMAs.

D. Other Components

A geared DC motors were used for the driving wheel. The motor model was D&J WITH's RA-12WGM series and the gear ratio was 1/298. The motor torque was transmitted to wheel by chain and gears. The wheel shaft was made by 3 mm carbon fiber square rod for easy assembly with the chain gear.

V. EXPERIMENTAL RESULTS

A. Wheel Stiffness Measure

The stiffness of the wheel is a key issue in the wheel design. Fig. 10 shows the experimental setup for the wheel stiffness measurement, and Fig. 11 shows the theoretical and experimental values of the relationship between the load and radius displacement of the wheel. In the experiment, a tensile tester (R&B Micro load RB302) was used for the displacement-force measurement. Wire was used to pull the structure: one end of the wire was attached to the tip of the wheel, and the other end was attached to the load cell of the

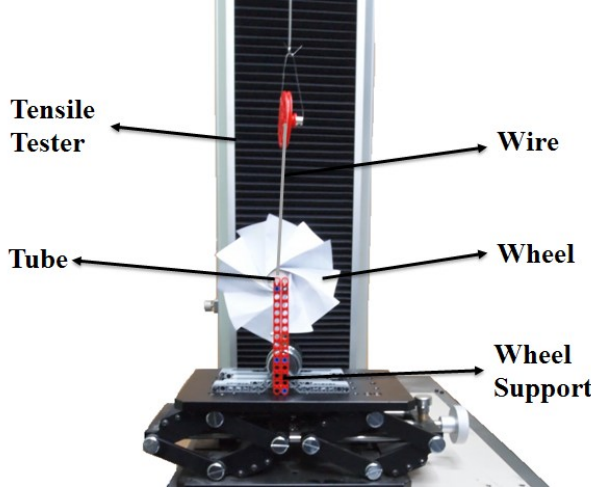
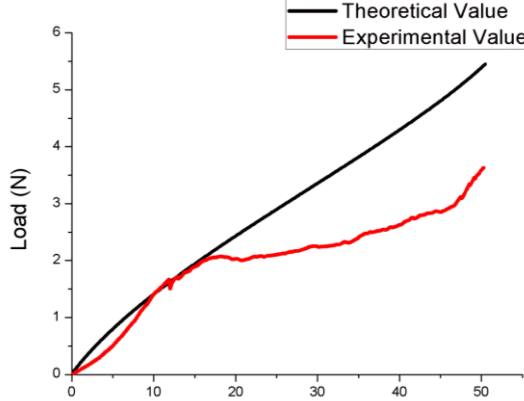


Figure 10. Experimental set-up for wheel stiffness measurement. Tensile tester, R&B Micro lad RB302 was used to measure the displacement-force relationship. One end of the wire was attached to the tip of the wheel, and the other end was attached to the load cell. To assure the direction of force always faced the center of the wheel, a tube was embedded in the center of the wheel, and the wire was passed though the tube.



tensile tester. To assure that the direction of the force always faced the center of the wheel, a tube was embedded in the center of the wheel, and the wire was passed though the tube. Because of the embedded plate springs, the whole structure moved like elastic body. The non-linearity of the result was due to the structure and compliance of the paper. The theoretical and experimental values matched fairly well at first, but buckling caused the stiffness of the wheel to dramatically decrease with large deformation. This phenomenon will be analyzed in future works.

B. Prototype Specification

The body size of the prototype was 15 cm x 10 cm, and the weight of the robot was 260 g including batteries. The diameter of the undeformed wheel was 11cm. The robot could drive at a maximum speed of 23 cm/s in the unfolded wheel state.

C. Deformation

When the wheels supported the weight of the robot, the wheel diameter in the unfolded state was 11 cm and it becomes 4 cm in the folded state. SMA activation required 1 s. The robot could pass through a 5 cm slit, which would be impossible if the wheel size could not be changed (Fig. 12).

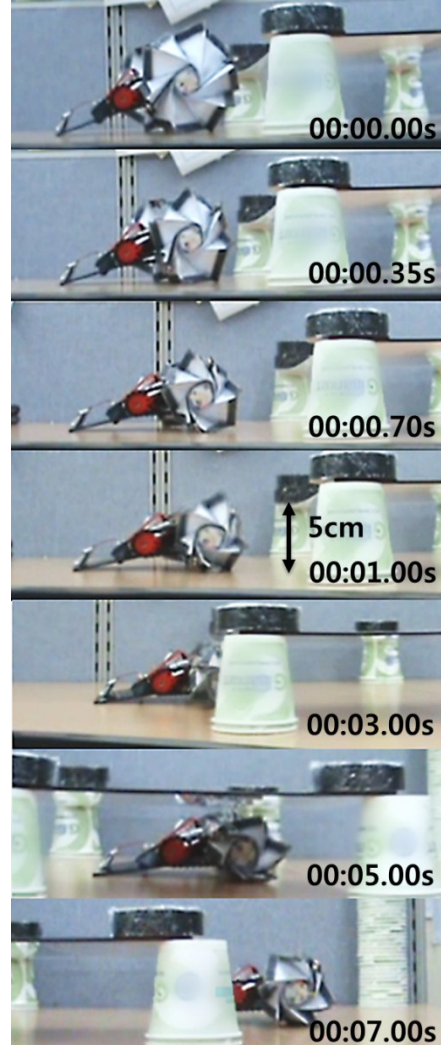


Figure 12. Prototype robot passing through a 5 cm slit. The picture demonstrates that the robot can pass through a slit that is smaller than the wheel size. The wheel size contracted from 11 cm to 4 cm, and then the robot can pass the 5 cm slit.

If one wheel is folded and the other remains unfolded, this unbalances the left and right wheel sizes; this allows for steering, as shown in Fig. 13. The robot's maximum steering ability was $1.2^\circ/\text{cm}$.

VI. CONCLUSION

This paper proposed a deformable wheeled robot based on an origami structure. The origami structure proposed by Guest *et al.* is used to replace a conventional linked mechanical system with a simple one-layer origami structure. The wheel can deform with only two plate springs and four SMA coil spring actuators. As a result, the wheel diameter of the robot can be reduced from 11cm to 4cm. Although the robot has an 11 cm wheel in its initial state, it can pass through 5 cm gaps by deformation. The wheel size can be selected depending on whether the large or small wheel is required.

There are still some issues that need to be resolved. First of all, clear analysis of the kinematic and the static models of

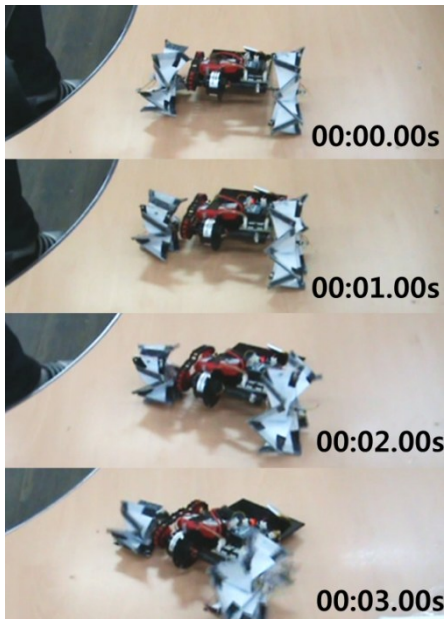


Figure 13. Robot can steer at a rate of $1.2^\circ/\text{cm}$ made possible by controlling the size of each wheel to be different. The pictures show the movement of the robot when only the right wheel is shrunk.

the wheel should be implemented. The model can be used to design the actuators and select the plated springs. The second issue is the material. The main body of the wheel was made by a paper; however, there are many candidate materials for origami structure that can increase the durability and performance of the wheel.

REFERENCES

- [1] H. C. Chiu, M. Rubenstein and W. M. Shen, "Deformable wheel – a self-recovering modular rolling track," *Distributed Autonomous Robotic Systems* 8, p. 429, 2009.
- [2] Y. Sugiyama and S. Hirai, "Crawling and jumping by a deformable robot", *The International Journal of Robotics Research*, Vol. 25, No. 5–6, pp 603–620, 2006.
- [3] S. Odedra, S. Prior, M. Karamanoglu and S. T. Shen, "Increasing the trafficability of unmanned ground vehicles through intelligent morphing", in *Proc. ASME/IFToMM Int. Conf. on Reconfigurable Mechanisms and Robots*, pp. 665-672, 2009.
- [4] E. Demaine, *Origami, linkages, and polyhedra: folding with algorithms*, Algorithms–ESA, 2006.
- [5] J. Justin, "Towards a mathematical theory of origami", in *Proc. the 2nd International Meeting of Origami Science and Scientific Origami*, pp. 15–29, 1994.
- [6] P. Jackson, *Folding Techniques for Designers: From Sheet to Form*, Pap/Cdr. Laurence King Publishers, 2011.
- [7] R. J. Lang, *Origami Design Secrets: Mathematical Methods for an Ancient Art, Second Edition*, A K Peters/CRC Press, 2011.
- [8] E. Hawkes, B. An, N. Benbernou, H. Tanaka, S. Kim, E. Demaine, D. Rus and R. Wood, "Programmable matter by folding", in *Proc. the National Academy of Sciences*, vol. 107, no. 28, p. 12441, 2010.
- [9] R. V. Martinez, C. R. Fish, X. Chen and G. M. Whitesides, "Elastomeric Origami: Programmable Paper-Elastomer Composites as Pneumatic Actuators", *Advanced Functional Materials*, vol. 22, pp. 1376–1384, 2012.
- [10] C. D. Onal, R. J. Wood and D. Rus, "Towards printable robotics: Origami-inspired planar fabrication of three-dimensional mechanisms", in *Proc. IEEE Int. Conf. on Robotics and Automation*, pp. 4608–4613, 2011.
- [11] N. Bassik, G. M. Stern and D. H. Gracias, "Microassembly based on hands free origami with bidirectional curvature", *Applied physics letters*, vol. 95, p. 091901, 2009.
- [12] P. O. Vaccaro, K. Kubota, T. Fleischmann, S. Saravanan and T. Aida, "Valley-fold and mountain-fold in the micro-origami technique", *Microelectronics journal*, vol. 34, no. 5–8, pp. 447–449, 2003.
- [13] T. TACHI, "Geometric Considerations for the Design of Rigid Origami Structures", in *Proc. the International Association for Shell and Spatial Structures Symposium*, 2010.
- [14] S. D. Guest and S. Pellegrino, "Inextensional wrapping of flat membranes", in *Proc. International Seminar on Structural Morphology, Montpellier*, pp 203–215. 1992.